

Children's Mercy Kansas City

**SHARE @ Children's Mercy**

---

Manuscripts, Articles, Book Chapters and Other Papers

---

5-2022

## **Utility of the $^{13}\text{C}$ -pantoprazole breath test as a CYP2C19 phenotyping probe for children**

Keith Feldman

Gregory L. Kearns

Robin E. Pearce

Susan M. Abdel-Rahman

J Steven Leeder

*See next page for additional authors*

Follow this and additional works at: <https://scholarlyexchange.childrensmercy.org/papers>

---

---

**Creator(s)**

Keith Feldman, Gregory L. Kearns, Robin E. Pearce, Susan M. Abdel-Rahman, J Steven Leeder, Alec Friesen, Vincent S. Staggs, Andrea Gaedigk, Jaylene Weigel, and Valentina Shakhnovich

---



## ARTICLE

# Utility of the <sup>13</sup>C-pantoprazole breath test as a CYP2C19 phenotyping probe for children

Keith Feldman<sup>1,2</sup> | Gregory L. Kearns<sup>3</sup> | Robin E. Pearce<sup>1,2</sup> |  
Susan M. Abdel-Rahman<sup>1,2</sup> | James Steven Leeder<sup>1,2</sup> | Alec Friesen<sup>4</sup> | Vincent S. Staggs<sup>1,2</sup> |  
Andrea Gaedigk<sup>1,2</sup> | Jaylene Weigel<sup>1</sup> | Valentina Shakhnovich<sup>1,2,5</sup>

<sup>1</sup>University of Missouri-Kansas City School of Medicine, Kansas City, Missouri, USA

<sup>2</sup>Children's Mercy Kansas City, Kansas City, Missouri, USA

<sup>3</sup>Texas Christian University and UNTHSC School of Medicine, Fort Worth, Texas, USA

<sup>4</sup>Oklahoma School of Community Medicine, Tulsa, Oklahoma, USA

<sup>5</sup>Center for Children's Healthy Lifestyles & Nutrition, Kansas City, Missouri, USA

## Correspondence

Valentina Shakhnovich, Children's Mercy Hospital, 2401 Gillham Rd., Kansas City, MO 64108, USA.  
Email: [vshakhnovich@cmh.edu](mailto:vshakhnovich@cmh.edu)

## Funding information

This work was supported by the NICHD-NIGMS T32 Training Program in Developmental/Pediatric Clinical Pharmacology (1T32HD069038; G.L.K.). V.S. received salary support from NIDDK (5K23DK115827; V.S.) during part of this work.

## Abstract

The <sup>13</sup>C-pantoprazole breath test (PAN-BT) is a safe, noninvasive, in vivo CYP2C19 phenotyping probe for adults. Our objective was to evaluate PAN-BT performance in children, with a focus on discriminating individuals who, according to guidelines from the Clinical Pharmacology Implementation Consortium (CPIC), would benefit from starting dose escalation versus reduction for proton pump inhibitors (PPIs). Children ( $n = 65$ , 6–17 years) genotyped for *CYP2C19* variants \*2, \*3, \*4, and \*17 received a single oral dose of <sup>13</sup>C-pantoprazole. Plasma concentrations of pantoprazole and its metabolites, and changes in exhaled <sup>13</sup>CO<sub>2</sub> (termed delta-over-baseline or DOB), were measured 10 times over 8 h using high performance liquid chromatography with ultraviolet detection and spectrophotometry, respectively. Pharmacokinetic parameters of interest were generated and DOB features derived using feature engineering for the first 180 min post-administration. DOB features, age, sex, and obesity status were used to run bootstrap analysis at each timepoint ( $T_1$ ) independently. For each iteration, stratified samples were drawn based on genotype prevalence in the original cohort. A random forest was trained, and predictive performance of PAN-BT was evaluated. Strong discriminating ability for CYP2C19 intermediate versus normal/rapid metabolizer phenotype was noted at DOB<sub>T<sub>30</sub> min</sub> (mean sensitivity: 0.522, specificity: 0.784), with consistent model outperformance over a random or a stratified classifier approach at each timepoint ( $p < 0.001$ ). With additional refinement and investigation, the test could become a useful and convenient dosing tool in clinic to help identify children who would benefit most from PPI dose escalation versus dose reduction, in accordance with CPIC guidelines.

This is an open access article under the terms of the [Creative Commons Attribution-NonCommercial-NoDerivs](https://creativecommons.org/licenses/by-nc-nd/4.0/) License, which permits use and distribution in any medium, provided the original work is properly cited, the use is non-commercial and no modifications or adaptations are made.

© 2022 The Authors. *Clinical and Translational Science* published by Wiley Periodicals LLC on behalf of American Society for Clinical Pharmacology and Therapeutics.

### Study Highlights

#### WHAT IS THE CURRENT KNOWLEDGE ON THE TOPIC?

*CYP2C19* genotype is a known determinant of drug disposition and response for proton pump inhibitors (PPIs). However, it is not the only determinant and genotype-phenotype discordance can occur.

#### WHAT QUESTION DID THIS STUDY ADDRESS?

Can the <sup>13</sup>C-pantoprazole breath test (PAN-BT) be utilized as a noninvasive *CYP2C19* phenotyping probe for children, and can the test discriminate the *CYP2C19* intermediate metabolizer (IM) phenotype (i.e., children who would benefit from PPI starting dose reduction) from the normal and rapid metabolizer (NM and RM) phenotype (i.e., children who would benefit from PPI starting dose escalation)?

#### WHAT DOES THIS STUDY ADD TO OUR KNOWLEDGE?

The PAN-BT can discriminate *CYP2C19* IMs from NMs and RMs in as little as 30 min (mean sensitivity 0.522, specificity 0.784), and is feasible in children as young as 6 years of age. Based on recently demonstrated receptiveness to drug dose individualization for PPIs in pediatrics, additional studies are warranted in pediatric populations.

#### HOW MIGHT THIS CHANGE CLINICAL PHARMACOLOGY OR TRANSLATIONAL SCIENCE?

A convenient, noninvasive, in-office, *CYP2C19* phenotyping probe could aid appropriate drug dose selection for PPIs in pediatrics.

## INTRODUCTION

Gastroesophageal reflux disease (GERD) affects approximately one in five people in North America, with an increasing prevalence noted over the past 25 years.<sup>1</sup> The efficacy of proton pump inhibitors (PPIs) in treating GERD and other gastrointestinal disorders (e.g., *Helicobacter pylori* gastritis and peptic ulcer disease) is well-established for both adult and pediatric patients. However, only recently have clinical guidelines been developed to help optimize and individualize PPI treatment based on an individual's genetic variation in *CYP2C19*, the major drug metabolizing pathway responsible for the biotransformation of most PPIs to inactive metabolites.<sup>2</sup> Based on newly published recommendations from the Clinical Pharmacology Implementation Consortium (CPIC), a large majority of patients (those with 2 functional copies of the *CYP2C19* allele, including normal function and gain-of-function alleles) would benefit from increasing the standard PPI starting dose by 50%–100% for efficacious treatment of several gastrointestinal disorders. The guidelines also recommend consideration of dose reduction for patients with one or two decreased or no function alleles (e.g., patients with a *CYP2C19*\*1/\*2, \*2/\*9, or \*3/\*4 genotype) if efficacy is achieved and chronic PPI therapy is anticipated.<sup>2</sup>

Although *CYP2C19* genotype is undoubtedly an important determinant of *CYP2C19* activity (i.e., phenotype), it is not the only determinant. *CYP2C19* phenotype is also

influenced by age.<sup>3</sup> Furthermore, *CYP2C19* genotype-phenotype discordance (sometimes referred to as phenoconversion) has been described as a consequence of diet, environment, liver disease, metabolic derangement, and concomitant medication use.<sup>4</sup> Highly relevant for individuals on chronic PPI therapy, *CYP2C19* phenoconversion is also common with chronic omeprazole/esomeprazole treatment in as little as 4 weeks of therapy, due to auto-inhibition of *CYP2C19* by these two PPI substrates.<sup>5,6</sup> Thus, a *CYP2C19* phenotyping, rather than a genotyping test, is perhaps of highest utility for patient care and clinical practice.

The <sup>13</sup>C-pantoprazole breath test (PAN-BT) was previously demonstrated to be a safe, effective, noninvasive, in vivo *CYP2C19* phenotyping test in adults.<sup>7,8</sup> For this test, the pantoprazole molecule is labeled with a stable, non-radioactive isotope of carbon (<sup>13</sup>C) at the methyl position and administered as a single oral dose. The labeled methyl group is cleaved by *CYP2C19*, liberating <sup>13</sup>CH<sub>4</sub>, which enters the body's carbon pool, gets converted to CO<sub>2</sub>, and is subsequently eliminated in exhaled air. The enrichment of <sup>13</sup>C in exhaled CO<sub>2</sub> over time is directly related to *CYP2C19* activity and can be measured using infrared spectrophotometry, which compares the baseline <sup>13</sup>CO<sub>2</sub>/<sup>12</sup>CO<sub>2</sub> ratio in an exhaled breath sample to changes in this ratio over time after <sup>13</sup>C-pantoprazole administration.<sup>7</sup>

Given that the noninvasive nature of this breath test is appealing for pediatric use, we evaluated PAN-BT performance in children. Specifically, we examined the ability

of PAN-BT to discriminate CYP2C19 phenotype (based on genotype) for children, and assessed the test's ability to capture interindividual variability in CYP2C19 activity independent of *CYP2C19* genotype.

## METHODS

### Study cohort and data collection

The data utilized for this study were collected as part of a prospective, single-center, pharmacokinetic (PK) study of pantoprazole (PAN) performed at the Children's Mercy Hospital (CMH) in Kansas City, MO (clinicaltrials.gov NCT01887743). The study was approved by the CMH Institutional Review Board and conducted in accordance with the ethical standards of the Declaration of Helsinki. In this secondary analysis of previously published PAN PK data,<sup>9</sup> we present new plasma metabolite and breath test data to help inform the relationship between the pharmacokinetics of PAN in plasma and CYP2C19 phenotyping using PAN-BT. The metabolites and breath test data presented herein have not been previously published.

After an overnight fast, children (6–17 years of age) with or without GERD and no other significant comorbidities, abstaining from drugs known to induce/inhibit CYP2C19, and not receiving concomitant therapy with PPIs, were enrolled during a 22-month period. Participants received a single oral dose of <sup>13</sup>C-PAN-sodium in bicarbonate solution (Cambridge Isotopes Laboratories), 1.2 mg/kg lean body weight (LBW), up to 100 mg maximum total dose. LBW was calculated using a validated equation.<sup>10</sup> Using high performance liquid chromatography with ultraviolet detection, as previously described for PPIs,<sup>11</sup> concentrations of PAN and its CYP2C19- and CYP3A4-mediated metabolites were quantified in plasma samples collected from an indwelling venous catheter (i.v.), prior to PAN administration and at 10 timepoints over 8 h after drug administration. The lower limit of detection for PAN, PAN-Sulfone, and PAN-N-oxide was 0.025 μM; for 4-desmethyl-PAN and PAN-sulfide 0.027 μM; for 4-desmethyl-PAN-sulfide-sulfate 0.023 μM; and for 4-desmethyl-PAN-sulfate and 4-desmethyl-PAN-sulfone-sulfate 0.022 μM. All analyses were performed in duplicate. PK profiles were generated using standard noncompartmental analysis (Kinetica version 5).

In addition to plasma samples, breath samples were collected using standard techniques previously described by our group<sup>12</sup> at predose and at 10, 20, 30, 40, 50, 60, 90, 120, and 180 min postdose to quantify concentrations of <sup>13</sup>CO<sub>2</sub> and <sup>12</sup>CO<sub>2</sub> in the air exhaled, using infrared spectrophotometry (POCone Spectrophotometer; Otsuka America Pharmaceutical). Enrichment of <sup>13</sup>CO<sub>2</sub> in breath

samples after study drug administration is the direct output of the spectrophotometer, expressed as the increase in the ratio of <sup>13</sup>CO<sub>2</sub>-to-<sup>12</sup>CO<sub>2</sub> relative to the baseline ratio at predose, termed the delta-over-baseline (DOB) value.

All participants were genotyped for the *CYP2C19* no-function (\*2, \*3, and \*4) and increased-function (\*17) alleles using commercially available TaqMan assays; details provided in Table S1. Allelic definitions are per PharmVar,<sup>13</sup> with genotype translated into phenotype groups recommended by the CPIC, as detailed in Table S1.

### Data analysis

Utilizing the collected data, we undertake a series of analyses to characterize CYP2C19 phenotype reflected in plasma pantoprazole PK and DOB, evaluate concordance of PAN-BT with established genotype-based CYP2C19 phenotypes, and assess the potential of PAN-BT to directly predict CYP2C19 phenotype independent of *CYP2C19* genotype. Details for each analysis can be found in the respective sections to follow, and a visual summary of each analysis can be found in [Figure 1](#).

### Association of CYP2C19 activity with genotype-based phenotype groups

In line with recent CPIC guidelines, the first section of this paper focuses on the comparison of CYP2C19 activity (measured as plasma PK and breath DOB) across established CYP2C19 phenotype groups based on *CYP2C19* genotype (i.e., CYP2C19 poor metabolizer [PM], intermediate metabolizer [IM], normal metabolizer [NM], rapid metabolizer [RM], and ultrarapid metabolizer [UM]). As expected, only a small number of children ( $n = 2$ ) in our cohort were homozygous for *CYP2C19* variant alleles; therefore, the one PM and one UM identified were excluded from statistical analyses. All subsequent analyses focus specifically on the cohort of IM and NM/RM children, as they represent the majority of the population. Based on the actionable dosing recommendations by CPIC to increase PPI starting dose by 50%–100% for both CYP2C19 NMs and RMs, these two phenotype groups were combined into a single study group (NM/RM).

Four distinct measures of CYP2C19 activity in plasma were compared for NM/RM versus IM. These included PAN total area under the concentration-time curve (AUC<sub>tot</sub>; μM per mg/kg), PAN apparent clearance (CL/F; L/h/kg total body weight), and the ratios of parent drug concentrations (PAN) to CYP2C19- and CYP3A4-mediated metabolite concentrations. For each measure, a series of summary statistics were computed, and nonparametric Mann-Whitney

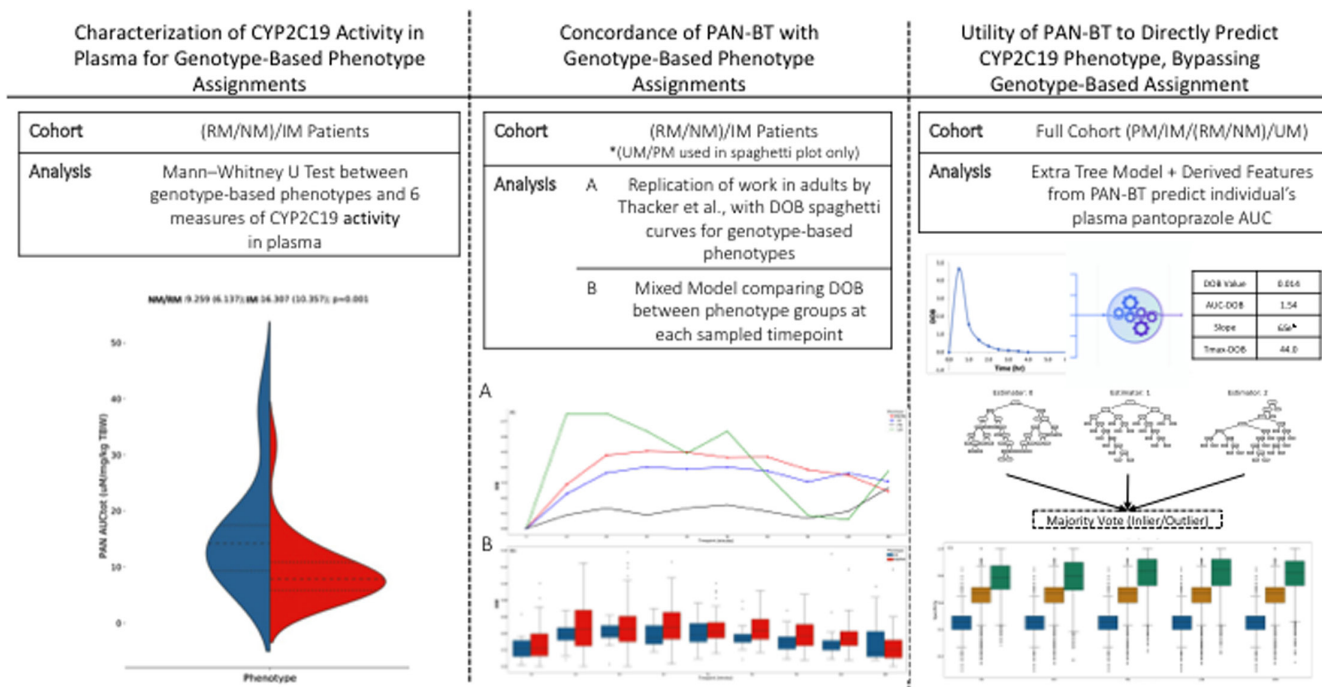


**FIGURE 1** Visual summary of the data analysis approaches performed and their anticipated results output. AUC, area under the concentration-time curve; DOB, delta-over-baseline; IM, intermediate metabolizer; NM, normal metabolizer; PAN-BT,  $^{13}\text{C}$ -pantoprazole breath test; PM, poor metabolizer; RM, rapid metabolizer; UM, ultrarapid metabolizer

$U$  tests were performed to assess for differences between genotype-based phenotypes and activity levels.

### Concordance of breath test with CYP2C19 phenotype groups based on genotype

Next, we undertook analyses to contextualize the relationship between data obtained from the PAN-BT and CYP2C19 genotype-based phenotype groups. First, we replicated work performed in adults by Thacker et al., which compared DOB values between genotype-based phenotypes at various timepoints.<sup>14</sup> Taking this comparison one step further, we explored nuance of inter-individual variability within each phenotype group. To quantitatively assess differences across the distributions, we performed a linear mixed model analysis, modeling DOB as a function of phenotype and time from baseline (20 min, 30 min, etc.). The model specification included a random patient intercept to account for clustering of repeated measures within each individual.  $T_0$  was excluded from this analysis, as DOB values at  $T_0$  were all 0 and did not add meaningful information. Given the small sample size for UM ( $n = 1$ ) and PM ( $n = 1$ ), comparisons were made exclusively between IM ( $n = 13$ ) and NM/RM ( $n = 46$ ). To aid in interpretation, visualizations via paired boxplots were created for each included genotype-based phenotype group at each sampled timepoint.

### Association of breath test features and CYP2C19 activity reflected in plasma PK

The final analysis of this paper explores bypassing the CYP2C19 phenotype assignments based on genotype, and instead assesses the potential of the PAN-BT to reflect plasma PAN PK and to predict CYP2C19 activity.

We began by constructing an augmented feature set designed to capture attributes of a patient's PAN-BT DOB curve. In addition to raw DOB value at each timepoint, three additional features (i.e., explanatory variables) were derived utilizing data up to and including the respective timepoint; these included area under the DOB curve, a line of best fit, and time to maximum concentration of the DOB. Details around the definition of each can be found in Table 1. Samples were also assigned a class label of *inlier* or *outlier* defined as those above or below the typical therapeutic PAN plasma  $\text{AUC}_{\text{tot}}$  after a 40 mg oral dose administration (i.e., 7–17  $\mu\text{M}$ ).<sup>15,16</sup> For participants missing a single breath sample ( $n = 4$ ), the missing DOB value was interpolated utilizing the Piecewise Cubic Hermite Interpolating Polynomial algorithm to account for the irregular shape of the DOB curve.<sup>17</sup> To facilitate comparisons across children receiving different total PAN doses (as dosing was weight-based and ranged from 20–100 mg), data were normalized by total drug dose received.

Utilizing the computed breath feature set, combined with demographic attributes shown to influence CYP2C19

**TABLE 1** Description of the derived breath test feature set

Feature	Definition
AUC-DOB	The total integrated area under the DOB curve provides a more precise representation of total CYP2C19 activity over time. To compute this value, the AUC is closely approximated from the set of discrete DOB values using the robust composite Simpson's rule. Given the unequal timepoints and nonlinear shape of the DOB curve, this approach was selected as it approximates each point among three adjacent points as a parabola.
Line of best fit	A line of best fit through the available data. Regression was used to model DOB at each timepoint as a function of elapsed time. Given the nonlinear nature of the data, a quadratic term for time was included in the model along with the linear term.
T <sub>max</sub> -DOB	Time of maximum DOB was converted to percentage of total time elapsed out of 180 min. Given the irregular shape of the curve, in the event that the maximum DOB value occurred at multiple time points, the earliest elapsed timepoint was used.

Abbreviations: AUC, area under the concentration-time curve; DOB, delta-over-baseline; T<sub>max</sub>, time of maximum concentration.

phenotype (age, sex, and weight status),<sup>15,18</sup> we built a 500-tree Extremely randomized Extra-Tree Forest to predict outlier status of each child.<sup>19</sup> Similar to random forests, Extra-Trees are an ensemble of single decision trees created using subsets of available features to improve generalizability. However, rather than using an optimal split criterion to grow the tree, each split is selected randomly, which has been shown to improve generalizability to unseen data when highly informative features (e.g., AUC) would dominate the split-order in any tree for which they were selected.

To estimate the expected performance of such a model, we utilized a robust bootstrap approach. Under the bootstrap paradigm, a sample of children was drawn with replacement until the size of the original dataset was reached, and stratified to preserve the prevalence of genotype-based phenotype categories of NM/RM, IM, and other (i.e., UM and PM) observed in the original cohort (i.e., bootstrap sample). By sampling with replacement, each bootstrap sample leaves out, on average, 37.8% of patients from the full cohort. These excluded cases (known as out-of-bag [OOB] samples) can then be used as test data on which to evaluate the performance of a model trained on the resampled data. The process was repeated for 10,000 iterations, and in the rare occurrence that no children in a bootstrap sample were labeled as outliers, a replacement bootstrap sample was drawn.

At each iteration, sensitivity, specificity, and F1 (harmonic mean of precision and recall) were computed for the OOB predictions. F1 results were reported as averages for inlier and outlier classes weighted by the class size. The performance of two baseline classifiers was also computed at each iteration: one which predicts the activity group (inlier/outlier) at random for each child, and one

that predicts accordingly with the observed population inlier/outlier distribution from the training cohort. All statistical analyses were completed using Python 3.7, Pandas 1.1.1, SkLearn 0.23, Numpy 1.19, and Scipy1.5.<sup>20-23</sup>

## RESULTS

Of the 71 children enrolled, 65 completed the study. Only those children who provided both evaluable DOB and plasma samples were included in this analysis ( $n = 61$ ). Of the four children excluded, two were excluded due to poor breathing techniques, one due to collection of less than 60% of the postdose breath samples, and one due to premature loss of i.v. for plasma collection. Characteristics of the remaining 61 participants are summarized in Table 2, and the comparison of their plasma PAN AUC<sub>tot</sub> as a function of CYP2C19 genotype is depicted in Figure 2. Adjusted for the mg/kg of the drug received, children with CYP2C19 \*1/\*2 genotype tended to have substantially higher plasma PAN AUC<sub>tot</sub> than children with \*1/\*1 or \*1/\*17 genotype ( $p < 0.015$ ), whereas children with \*1/\*1 and \*1/\*17 genotypes had no statistically significant differences in PAN AUC<sub>tot</sub> ( $p = 0.561$ ). Together, \*1/\*2, \*1/\*1, and \*1/\*17 genotypes accounted for 95% of our patient cohort.

The violin plots in Figure 3 highlight the distribution of children with the NM/RM and IM CYP2C19 phenotype assignments (based on genotype) across six primary CYP2C19 activity measurements in plasma: PAN AUC<sub>tot</sub>, PAN CL/F, and PAN-to-metabolite ratios for CYP2C19-mediated metabolites (i.e., 4-desmethyl-PAN and 4-desmethyl-PAN-sulfate), and CYP3A4-mediated metabolites (i.e., PAN-Sulfone and PAN-Sulfide). To account for contribution of metabolites formed as a

**TABLE 2** Study cohort characteristics

	Mean (SD)	Range
Age, years	13.81 (3.36)	[6.08–17.92]
Weight, kg	61.71 (21.57)	[18.50–124.00]
BMI z-score	1.07 (0.84)	[−0.92–2.83]
BMI %	79.27 (20.07)	[18.00–99.80]
PAN dose, mg	50.42 (15.89)	[16.5–88]
Sex	<b>n (%)</b>	
Male	26 (42.62)	
Female	35 (57.38)	
Race or ethnicity	<b>n (%)</b>	
White	42 (68.85)	
African American	11 (18.03)	
Hispanic	6 (9.84)	
Mixed	2 (3.28)	
	<b>PAN plasma AUC<sub>tot</sub> (μM per mg/kg TBW)</b>	
<b>Genotype</b>	<b>n (%)</b>	<b>Mean (SD) Range</b>
*17*17	1 (1.64)	4.18 (–) –
*1*1	30 (49.18)	10.04 (6.81) [2.68–33.75]
*1*17	16 (26.23)	7.84 (4.52) [2.26–18.59]
*2*17	3 (4.91)	10.42 (3.40) [7.71–14.23]
*1*2	10 (16.40)	18.07 (11.20) [7.36–41.31]
*2*2	1 (1.64)	226.59 (–) –

Abbreviations: AUC<sub>tot</sub>, total area under the concentration-time curve; BMI, body mass index; PAN, pantoprazole; TBW, total body weight.

consequence of both CYP2C19 and CYP3A4 activity (i.e., 4-desmethyl-PAN-sulfone-sulfate and 4-desmethyl l-PAN-sulfide-sulfate), these metabolite concentrations were alternatively counted toward total CYP2C19 activity (Figure 3e) or total CYP3A4 activity (Figure 3f). In addition to significantly increased plasma PAN AUC<sub>tot</sub> and significantly decreased PAN CL/F ( $p = 0.001$ ; Figure 3a,b), plasma ratios of PAN to CYP2C19-mediated metabolites were significantly higher in NM/RM versus IM ( $p \leq 0.001$ ; Figure 3c,e). Although the ratio of PAN to CYP3A4-mediated metabolites was slightly higher in NM/RM versus IM, this difference did not reach statistical significance ( $p \geq 0.198$ ; Figure 3d,f).

### Concordance of breath test with CYP2C19 phenotype assignments based on genotype

Having established significant differences in CYP2C19 activity between NM/RM and IM in plasma (Figure 3), Figure 4a presents the mean DOB values at each sampled timepoint for the four CYP2C19 phenotype groups

based on genotype. As expected, we observe a nearly monotonical increase in early DOB values as a function of functional/suprafucional alleles (i.e., from PM → IM → EM → UM).

Taking this one step further, in Figure 4b, we display interindividual variability (and subsequent observed degree of overlap) within the NM/RM and IM phenotype assignments. To quantify this overlap, our repeated measures mixed model assessed the average difference between NM/RM and IM (referent). Although differences appeared minimal ( $\beta$  95% confidence interval: [−0.004–0.017],  $p = 0.26$ ), individuals in the NM/RM group tended to have higher means at several timepoints. Nonetheless, the range of values for the IM group was found to nearly or completely overlap with the range of values in the NM/RM group.

### Association of breath test features and CYP2C19 activity reflected in plasma PK

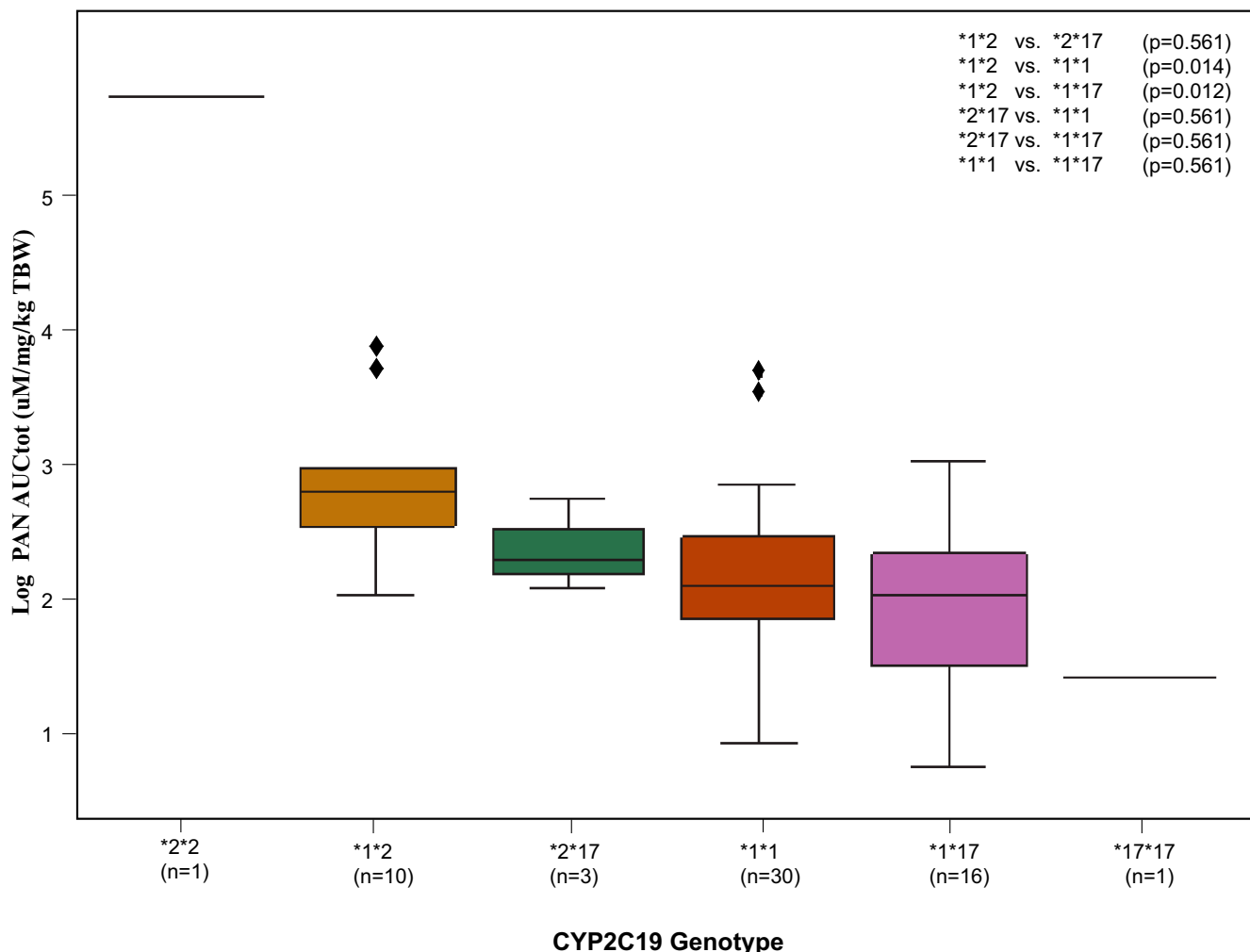
Given the observed degree of overlap in DOB between the NM/RM and IM groups, our final analysis focused on use of PAN-BT to directly predict the expected CYP2C19 activity without consideration of pre-assigned phenotype labels based on CYP2C19 genotype. Specifically, we focused on the prediction of those patients who fall outside the typical PAN plasma AUC<sub>tot</sub> range previously associated with therapeutic response (7–17 μM).<sup>15,16</sup>

Figure 5 presents the sensitivity, specificity, and F1 performance distributions over the 10,000 bootstrap iterations at each DOB timepoint. The DOB derived features from PAN-BT illustrate improved performance over the stratified dummy classifier (Wilcoxon signed-rank test  $p < 0.001$  between each iteration repeated at each timepoint adjusted for multiple comparisons). Notably, the random classifier outperformed the model-based approach, particularly at the later timepoints in terms of sensitivity. However, this phenomenon is simply a result of the random overclassifying of outliers (i.e., increased false-positive results). We can reaffirm this looking at the F1 score, where the negative class is weighted by the class size. Again, we find the proposed model using PAN-BT to outperform both the stratified and random classifiers ( $p < 0.001$ ). For completeness, we also inspected the class-wise recall rate and confirmed that the random classifier had the lowest inlier-recall values.

## DISCUSSION

Similar to previous findings in adults, our data demonstrate that PAN-BT can be used in children to discriminate





**FIGURE 2** Plasma pantoprazole (PAN) AUC<sub>tot</sub> as a function of *CYP2C19* genotype. AUC<sub>tot</sub> data are adjusted for mg/kg drug received and log-transformed. Pairwise comparisons across genotype groups are reported in the figure legend with statistically significantly lower AUC<sub>tot</sub> observed in *CYP2C19* \*1\*2 compared to \*1\*1 or \*1\*17 individuals ( $p < 0.015$ ,  $\alpha < 0.05$ , adjusted for multiple comparisons with Holm step-down procedure). Individuals genotyped as *CYP2C19* \*2\*2 ( $n = 1$ ) and \*17\*17 ( $n = 1$ ) were excluded from statistical analysis. Horizontal line in box-whisker plots represents the median, with whiskers denoting the interquartile range (IQR) and diamonds corresponding to values greater than 1.5 times outside the IQR. AUC<sub>tot</sub>, total area under the concentration-time curve

individuals with two functional *CYP2C19* alleles (i.e., NM/RM genotype-based phenotype) from individuals with one functional allele (i.e., IM genotype-based phenotype) in a timespan as short as 1 h (e.g., mean sensitivity 0.522 and specificity 0.784 at 30 min). This finding is clinically important because new *CYP2C19* genotype-based PPI dosing guidelines from the CPIC advocate for 50%–100% escalation of the standard PPI starting dose for *CYP2C19* NM/RMs for certain conditions (e.g., erosive esophagitis), and consideration of 50% PPI dose reduction for IMs. As recently demonstrated in a multicenter, pragmatic, pediatric trial of genotype-guided PPI dose selection, both patients and prescribers are ready to embrace such precision dosing for PPIs, and willing to wait up to 2 weeks for genotyping results prior to starting therapy.<sup>24</sup> PAN-BT could offer a convenient, noninvasive, in-office precision dosing

tool alternative, with more quickly and readily available results. DOB is the direct output of spectrophotometry equipment that is already readily available at many hospitals and clinics for other routine clinical testing (e.g., urea breath test for *Helicobacter pylori* and lactulose breath test for small bowel bacterial overgrowth). Administering an oral dose of <sup>13</sup>C-PAN to children about to be prescribed a PPI for clinical indications, collecting a sample of exhaled air predose and postdose (at the end of a clinical visit, for example), and running the breath sample through a spectrophotometer on site should therefore, theoretically, pose few logistical barriers for implementation. However, we fully acknowledge that additional research is necessary before steps can be taken to implement the test for clinical purposes. Although formal statistical analysis to assess PAN-BT's capacity to discriminate UM and PM *CYP2C19*

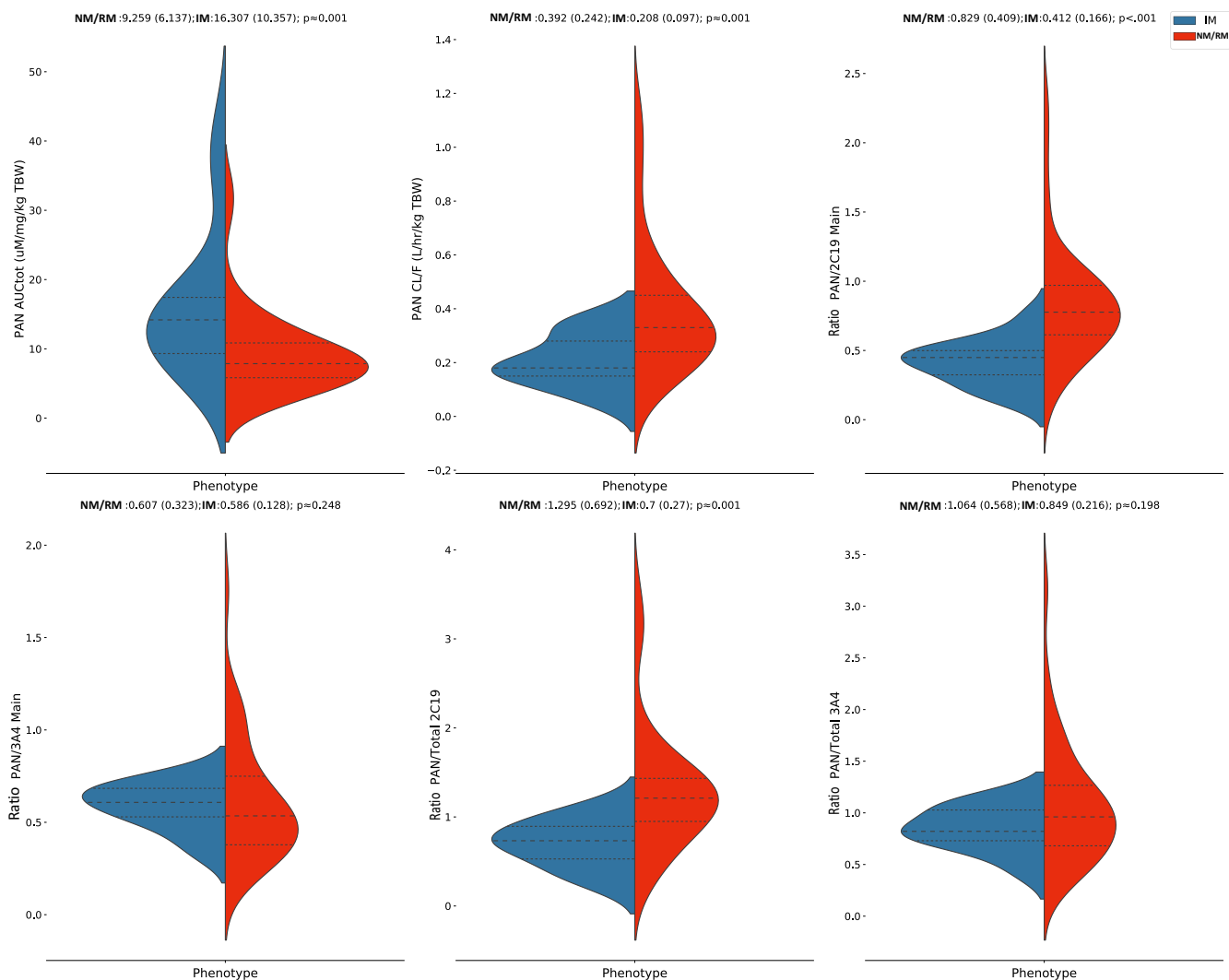


**FIGURE 3** Violin plots of CYP2C19 activity measures in plasma for individuals with the intermediate metabolizer (IM; blue) CYP2C19 genotype-based phenotype versus the normal metabolizer and rapid metabolizer genotype-based phenotype (NM/RM; orange). Dashed lines in violin plots represent the mean (---) and standard deviation (---) for each plasma activity measure. The mean and standard deviation values are provided in the figure panel titles, with comparisons between CYP2C19 NM/RM and IM made using the Mann-Whitney  $U$  test ( $\alpha < 0.05$ ). Activity measures per panel include (a) AUC<sub>tot</sub> for pantoprazole (PAN) adjusted for mg/kg drug received; (b) apparent oral clearance for PAN (CL/F); (c-f) PAN-to-metabolite ratios where 4-desmethyl-PAN and 4-desmethyl-PAN-sulfate represent the main CYP2C19-mediated metabolites (2C19 Main; panel c), PAN-Sulfone and PAN-Sulfide the main CYP3A4-mediated metabolites (3A4 Main; panel d), and 4-desmethyl-PAN-sulfone-sulfate and 4-desmethyl-PAN-sulfide-sulfate metabolites formed as a byproduct of combined activity from both CYP2C19 and CYP3A4. To capture total CYP activity, these latter “combination” metabolites were summed with the main CYP2C19 metabolites (Total 2C19; panel e), or with the main CYP3A4 metabolites (Total 3A4; panel f). AUC, area under the concentration-time curve

phenotypes could not be performed in our study due to the small sample size ( $n = 2$ ), visual inspection of DOB curves in [Figure 4a](#) suggests that this may be possible within a timeframe as short as 30 min.

One added advantage of PAN-BT over genotyping is the test’s ability to capture real-time, CYP2C19 activity in vivo, which, in addition to CYP2C19 genotype, is influenced by factors such as age, diet, concomitant medication use, etc.<sup>4</sup> Thus, the test is ideally suited to account for the relevant, real-world sources of interindividual

variability in CYP2C19 activity not captured by genotype alone. Indeed, measures of CYP2C19 activity in plasma ([Figure 3](#)) and breath samples ([Figure 5b](#)) in our study showed a substantial degree of overlap across the conventional phenotype groups based on CYP2C19 genotype (i.e., RM/NM/IM). For this reason, in addition to evaluating the accuracy of genotype-based phenotype, we elected to apply PAN-BT to predict individuals whose plasma PAN AUC<sub>tot</sub> would fall outside of the typical therapeutic range associated with a standard 40 mg oral

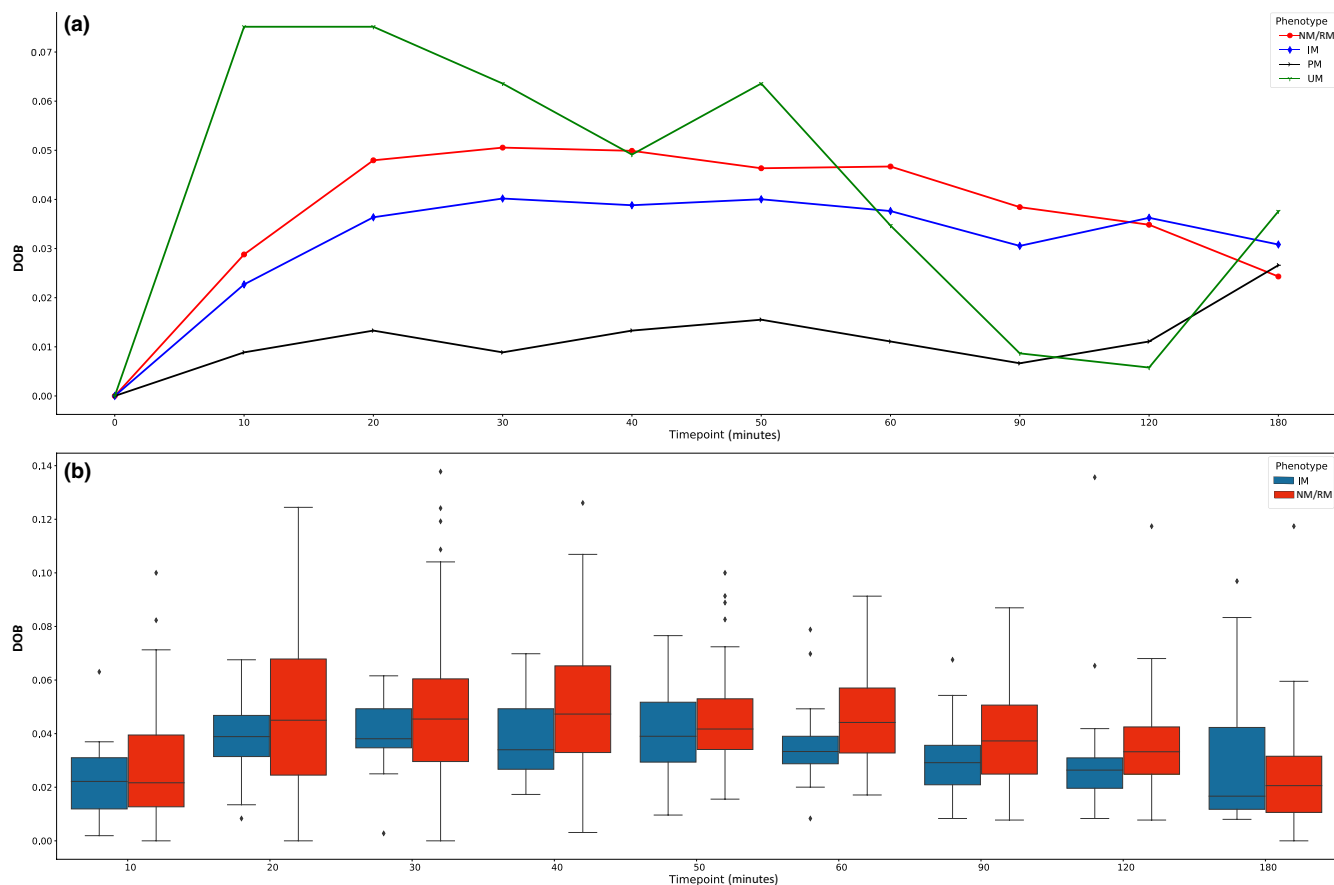


**FIGURE 4** Relative enrichment of <sup>13</sup>C in expired CO<sub>2</sub> (termed delta-over-baseline [DOB]) over 3 h, after pantoprazole breath test administration. Although, the mean DOB values illustrate logical increases from PM → IM → EM → UM (a), there is a significant overlap across phenotypes when considering individual-level variance at each timepoint (b). No statistical difference ( $\alpha < 0.05$ ) in the group's mean DOB across timepoints was found using linear-mixed model with patient random intercepts. IM, intermediate metabolizer; NM, normal metabolizer; PM, poor metabolizer; RM, rapid metabolizer; UM, ultrarapid metabolizer

dose of pantoprazole (Figure 5). Given the large number of bootstrap iterations performed, this model-based approach using PAN-BT is expected to outperform a random selection based on the expected outlier rates seen in the general population (i.e., what is currently practiced at the bedside). Presumably, it is these outlier patients whose systemic drug exposures fall above or below the therapeutic range from a standard PPI dose, who would benefit most from PPI dose adjustment, independent of their *CYP2C19* genetic makeup.

Evidence is mounting that systemic PPI drug concentrations outside the therapeutic range are not as benign as once thought. Subtherapeutic exposures can result in therapeutic failure to eradicate *H. pylori* infection or heal erosions from acid damage, for example.<sup>2</sup> Conversely, supratherapeutic exposures, especially over a prolonged period of time, can lead to increased risk of adverse events, such as kidney disease,<sup>25</sup> osteopenia and mineral deficiencies,<sup>26,27</sup> and enteral and respiratory infections, particularly in children.<sup>27,28</sup> In a pilot, genotype-guided,

pragmatic trial, Cicali and colleagues recently demonstrated comparable PPI efficacy and a trend toward fewer respiratory adverse events in children ( $p = 0.07$ ) over a 12-week treatment course for GERD, when PPI dose selection was informed by *CYP2C19* genotype compared to a conventional “one-dose-fits-all” dosing approach.<sup>24</sup> A phenotype-based dosing approach using PAN-BT can be expected to offer comparable benefit, with the added advantage of accounting for genotype-phenotype discordance secondary to disease, dietary components or concomitant medications competing for *CYP2C19*-mediated metabolism, and/or auto-inhibition of *CYP2C19* from chronic PPI therapy. Thus, further research to establish PAN-BT DOB reference ranges to inform drug dose selection across the PPI drug class are warranted. This is especially true for pediatrics, where patients and prescribers are ready for a shift in the traditional PPI dosing paradigm toward individualized precision dosing, as illustrated in the pragmatic trial by Cicali et al.<sup>24</sup>

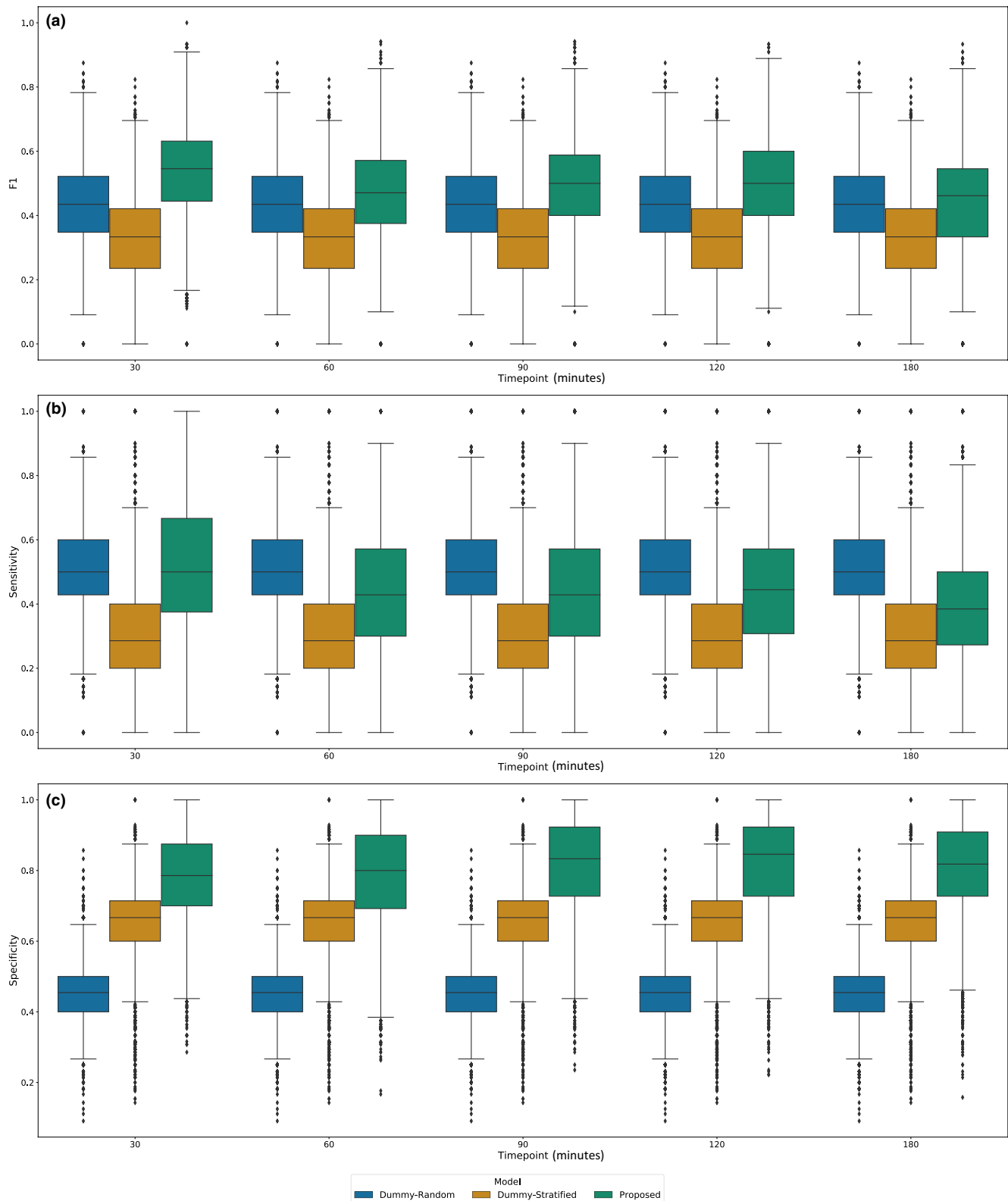


**FIGURE 5** Predictive performance of the  $^{13}\text{C}$ -pantoprazole breath test on outlier prediction for plasma pantoprazole (PAN)  $\text{AUC}_{\text{tot}}$  adjusted for mg/kg drug received, (a) sensitivity, (b) specificity, and (c) harmonic mean of precision and recall (F1). Boxplots represent score distributions across the 10,000 bootstrap iterations. Horizontal line represents the median performance, with whiskers denoting the interquartile range (IQR). Models evaluated included a completely random classifier (blue), a stratified random classifier based on overall outlier proportion in the training data (orange), and the Extra-Tree model with breath test delta-over-baseline (DOB) and derived features (green). Performance to the stratified random classifier was compared at each iteration using nonparametric Wilcoxon signed-rank test and found to be significant ( $\alpha < 0.05$ , adjusted for multiple comparisons with Holm step-down procedure)

## Study limitations

To our knowledge, our study represents the first published pediatric experience with the PAN-BT; however, as with any study, it has limitations. Although our preliminary results are strong, the generalizability of the predictive values and association magnitudes is limited by overall sample size. Confirmatory studies aimed at evaluating performance with improved precision will require larger diverse patient cohorts. This diversity will be essential to expand phenotype comparison from the UM ( $n = 1$ ) and PM ( $n = 1$ ) assignments based on *CYP2C19* genotype. Given that our study population is primarily (>85%) White and African American, the observed prevalence of these phenotypes is in line with the expected population prevalence (~ 2%) based on race/ethnicity.<sup>29</sup>

Additional limitations may include our decision to combine children with the *CYP2C19* \*1\*1 and \*1\*17 genotypes into a single study group. However, this decision was made deliberately because the actionable CPIC recommendation to increase the PPI starting dose by 50%–100% is the same for *CYP2C19* \*1\*1 and \*1\*17 individuals.<sup>2</sup> Last, some children in our study had trouble mastering the breathing technique for PAN-BT, which likely contributed to the irregularity of the DOB curves, necessitating additional processing of the DOB data directly outputted by the spectrophotometer. More broadly, prospective assessment of the test's utility in guiding dosing decisions across the PPI drug class are needed before the test could be implemented as a precision dosing tool in the clinic. However, collection of such data is promising as, with proper coaching, 97% of children were ultimately successful in providing adequate DOB data.

## CONCLUSIONS

Our study supports the assertion that the PAN-BT could provide a clinically useful, noninvasive method for assessing *CYP2C19* activity (i.e., phenotype) in children. Our results confirm the feasibility of test administration to children as young as 6 years of age with some coaching, and demonstrate comparable test performance to adult studies for distinguishing the *CYP2C19* NM/RM genotype-based phenotype from IM. If administered in the clinic, this test could potentially identify children who would benefit from PPI dose escalation versus dose reduction in as little as 1 h. In our opinion, a phenotype-based PPI dosing strategy using the PAN-BT could offer added benefit over a genotype-based strategy, as it would account for *CYP2C19* genotype-phenotype discordance from diet, disease, concomitant medication use, and/or

auto-inhibition of *CYP2C19* by chronic PPI therapy. Based on the willingness of pediatric patients, parents, and providers to participate in a recent, pragmatic, clinical trial of PPI drug dose individualization,<sup>24</sup> the timing may be ideal for further investigation of the utility of the PAN-BT in pediatrics.

## ACKNOWLEDGEMENTS

The authors would like to thank summer scholars Megan Buri, MD, and Richard Thompson, DO, for their help with sample collection, as well as Anil Modak, PhD, and Cambridge Isotopes Laboratories (Cambridge, MA) for providing the study drug. We would also like to thank Karim Pirani, PhD, for his assistance with genotyping.

## CONFLICT OF INTEREST

The authors declared no competing interests for this work.

## AUTHOR CONTRIBUTIONS

All authors wrote the paper. V.S., G.L.K., and J.S.L. designed the research. V.S., J.W., R.E.P., and A.F. performed the research. V.S., K.F., R.E.P., S.A.-R., and V.S.S. analyzed the data. K.F., R.E.P., S.A.-R., V.S.S., and A.G. contributed new reagents/analytical tools.

## REFERENCES

1. El-Serag HB, Sweet S, Winchester CC, Dent J. Update on the epidemiology of gastro-oesophageal reflux disease: a systematic review. *Gut*. 2014;63:871-880.
2. Lima JJ, Thomas CD, Barbarino J, et al. Clinical Pharmacogenetics Implementation Consortium (CPIC) guideline for *CYP2C19* and proton pump inhibitor dosing. *Clin Pharm Ther*. 2021;109:1417-1423.
3. Jin Y, Pollock BG, Frank E, et al. Effect of age, weight, and *CYP2C19* genotype on escitalopram exposure. *J Clin Pharmacol*. 2010;50:62-72.
4. Modak AS. Point-of-care companion diagnostic tests for personalizing psychiatric medications: fulfilling an unmet clinical need. *J Breath Res*. 2017;12: 017101.
5. Klieber M, Oberacher H, Hofstaetter S, et al. *CYP2C19* phenocconversion by routinely prescribed proton pump inhibitors omeprazole and esomeprazole: clinical implications for personalized medicine. *J Pharmacol Exp Ther*. 2015;354:426-430.
6. Harvey A, Modak A, Déry U, et al. Changes in *CYP2C19* enzyme activity evaluated by the [<sup>13</sup>C]-pantoprazole breath test after co-administration of clopidogrel and proton pump inhibitors following percutaneous coronary intervention and correlation to platelet reactivity. *J Breath Res*. 2016;10:017104.
7. Desta Z, Modak A, Nguyen PD, et al. Rapid identification of the hepatic cytochrome P450 2C19 activity using a novel and non-invasive [<sup>13</sup>C] pantoprazole breath test. *J Pharmacol Exp Ther*. 2009;329:297-305.
8. Furuta T, Kodaira C, Nishino M, et al. [<sup>13</sup>C]-pantoprazole breath test to predict *CYP2C19* phenotype and efficacy of a proton pump inhibitor, lansoprazole. *Aliment Pharmacol Ther*. 2009;30:294-300.

9. Shakhnovich V, Abdel-Rahman S, Friesen CA, et al. Lean body weight dosing avoids excessive systemic exposure to proton pump inhibitors for children with obesity. *Pediatr Obes*. 2019;14:e12459.
10. Janmahasatian S, Duffull SB, Ash S, Ward LC, Byrne NM, Green B. Quantification of lean bodyweight. *Clin Pharmacokinet*. 2005;44:1051-1065.
11. Aoki I, Okumura M, Yashiki T. High-performance liquid chromatographic determination of lansoprazole and its metabolites in human serum and urine. *J Chromatogr B Biomed Appl*. 1991;571:283-290.
12. Leeder JS, Pearce RE, Gaedigk A, Modak A, Rosen DI. Evaluation of a [<sup>13</sup>C]-dextromethorphan breath test to assess CYP2D6 phenotype. *J Clin Pharmacol*. 2008;48:1041-1051.
13. Botton MR, Whirl-Carrillo M, Del Tredici AL, et al. PharmVar GeneFocus: CYP2C19. *Clin Pharmacol Ther*. 2021;109:352-366.
14. Thacker DL, Modak A, Flockhart DA, Desta Z. Is (+)-[<sup>13</sup>C]-pantoprazole better than (±)-[<sup>13</sup>C]-pantoprazole for the breath test to evaluate CYP2C19 enzyme activity? *J Breath Res*. 2012;7:016001.
15. Shakhnovich V, Brian Smith P, Guptill JT, et al. A population-based pharmacokinetic model approach to pantoprazole dosing for obese children and adolescents. *Pediatr Drugs*. 2018;20:483-495.
16. Knebel W, Tammara B, Udata C, Comer G, Gastonguay M, Meng X. Population pharmacokinetic modeling of pantoprazole in pediatric patients from birth to 16 years. *J Clin Pharmacol*. 2011;51:333-345.
17. Fritsch FN, Carlson RE. Monotone piecewise cubic interpolation. *SIAM J Numer Anal*. 1980;17:238-246.
18. Ward RM, Kearns GL, Tammara B, et al. A multicenter, randomized, open-label, pharmacokinetics and safety study of pantoprazole tablets in children and adolescents aged 6 through 16 years with gastroesophageal reflux disease. *J Clin Pharmacol*. 2011;51:876-887.
19. Geurts P, Ernst D, Wehenkel L. Extremely randomized trees. *Mach Learn*. 2006;63:3-42.
20. McKinney W. *Data Structures for Statistical Computing in Python*. Proceedings of the 9th Python in Science Conference; 2010: 51-56.
21. Pedregosa F, Varoquaux G, Gramfort A, et al. Scikit-learn: machine learning in Python. *J Mach Learn Res*. 2011;12:2825-2830.
22. Harris CR, Millman KJ, van der Walt SJ, et al. Array programming with NumPy. *Nature*. 2020;585:357-362.
23. Virtanen P, Gommers R, Oliphant TE, et al. SciPy 1.0: fundamental algorithms for scientific computing in Python. *Nat Methods*. 2020;17:261-272.
24. Cicali EJ, Blake K, Gong Y, et al. Novel implementation of genotype-guided proton pump inhibitor medication therapy in children: a pilot, randomized, multisite pragmatic trial. *Clin Transl Sci*. 2019;12:172-179.
25. Jaynes M, Kumar A. The risks of long-term use of proton pump inhibitors: a critical review. *Ther Adv Drug Saf*. 2019;10:2042098618809927.
26. Thong BKS, Ima-Nirwana S, Chin K-Y. Proton pump inhibitors and fracture risk: a review of current evidence and mechanisms involved. *Int J Environ Res Public Health*. 2019;16:1571.
27. Bernal CJ, Aka I, Carroll RJ, et al. CYP2C19 phenotype and risk of proton pump inhibitor-associated infections. *Pediatrics*. 2019;144:e20190857.
28. Lima JJ, Lang JE, Mougey EB, et al. Association of CYP2C19 polymorphisms and lansoprazole-associated respiratory adverse effects in children. *J Pediatr*. 2013;163:686-691.
29. PharmGKB. Gene-specific information tables for CYP2C19. <https://www.pharmgkb.org/page/cyp2c19RefMaterials>; Accessed September 21, 2021.

## SUPPORTING INFORMATION

Additional supporting information may be found in the online version of the article at the publisher's website.

**How to cite this article:** Feldman K, Kearns GL, Pearce RE, et al. Utility of the <sup>13</sup>C-pantoprazole breath test as a CYP2C19 phenotyping probe for children. *Clin Transl Sci*. 2022;15:1155-1166. doi:[10.1111/cts.13232](https://doi.org/10.1111/cts.13232)